# Oxidation of cathepsin S by major chemicals of cigarette smoke

Mylène Wartenberg, Pierre-Marie Andrault, Ahlame Saidi, Paul Bigot, Lydie Nadal-Desbarats, Fabien Lecaille, Gilles Lalmanach

# Oxidation of cathepsin S by major chemicals of cigarette smoke

**Mylène Wartenberg [1,2], Pierre-Marie Andrault [1,2 *], Ahlame Saidi [1,2], Paul Bigot [1,2], Lydie Nadal-Desbarats [1,3], Fabien Lecaille [1,2], Gilles Lalmanach [1,2 **]**

[1] Université de Tours, Tours, France

[2] INSERM, UMR1100, Centre d'Etude des Pathologies Respiratoires (CEPR), Team « Mécanismes Protéolytiques dans l'Inflammation », Tours, France

[3] INSERM, UMR1253, Imagerie et Cerveau (iBrain), Team « Imageries, Biomarqueurs et Thérapies », Tours, France.

[*] Current address: Department of Oral Biological and Medical Sciences, University of British Columbia, Vancouver (BC), Canada

[**] Corresponding author: Gilles Lalmanach

INSERM UMR1100, Centre d'Etude des Pathologies Respiratoires (CEPR)

Team « Mécanismes Protéolytiques dans l'Inflammation »

Université de Tours, Faculté de Médecine

10 Boulevard Tonnellé, 37032 Tours cedex, France

Tel : (+33) 2 47 36 61 51 – Mail : gilles.lalmanach@univ-tours.fr

## **Abstract** *(242 words)*

Lung cysteine cathepsin S (CatS) that is a potent elastase plays a deleterious role in alveolar remodeling during smoke-induced emphysema. Despite the presence of a reactive nucleophilic cysteine (Cys25) within its active site, most of its elastinolytic activity is preserved after exposure to cigarette smoke extract (CSE), a major source of sulfhydryl oxidants. This result led us to decipher CatS resistance to major and representative CSE oxidants: hydrogen peroxide, formaldehyde, acrolein and peroxynitrite. CatS was inactivated by hydrogen peroxide, peroxynitrite and acrolein in a time- and dose-dependent manner, while formaldehyde was a weaker oxidant. Hydrogen peroxide, but not CSE, formaldehyde, and peroxynitrite impaired the autocatalytic maturation of pro-CatS, whereas acrolein prevented the formation of mature CatS without hindering the initial step of the two-step autocatalytic process. Far-UV CD spectra analysis supported that oxidation by CSE and hydrogen peroxide did not led to a structural alteration of CatS, despite a notable increase of protein carbonylation, a major hallmark of oxidative damage. Evaluation of the oxidation status of Cys25 by specific biotinylated redox sensing probes suggested the formation of sulfenic acid followed by a slower conversion to sulfinic acid after incubation with hydrogen peroxide. Addition of reducing reagents (dithiothreitol, glutathione and N-acetyl cysteine) led to a partial recovery of CatS activity following incubation with CSE, hydrogen peroxide and peroxynitrite. Current results provide some mechanistic evidence of CatS stability and activity in the presence of CSE, supporting its harmful contribution to the pathophysiology of emphysema.

**Abbreviations:**

Ahx: 6-aminohexanoic acid; AMC: 7-amino-4-methyl coumarin; BALF, bronchoalveolar lavage fluid; BP1: biotin-1,3-cyclopentanedione; Brij35: polyethylene glycol lauryl ether; BSA: bovine serum albumin; CatS: cathepsin S; CD: circular dichroism; COPD: chronic obstructive pulmonary disease; CS: cigarette smoke; CSE: cigarette smoke extract; DMK: diazomethylketone; DNP: 2,4-Dinitrophenol; DNPH: dinitrophenylhydrazine; DTT: DL-dithiothreitol; E-64: 3-epoxy-propionyl-leucylamide-(4-guanido)-butane; ECL: enhanced chemiluminescence; ECM: extracellular matrix; EDTA: ethylene diamine tetra acetic acid; FA: formaldehyde; GSH: glutathione; $H_2O_2$: hydrogen peroxide; HEPES: 4-(2-hydroxyethyl)-1-piperazineethanesulfonic acid; IFN: interferon; IL: interleukin; MAPK: mitogen-activated protein kinases; NMR: nuclear magnetic resonance; NO: nitric oxide; NO-Bio: phenyl 4-((5,21-dioxo-1-(2-oxohexahydro-1*H*-thieno[3,4-*d*]imidazol-4-yl)-9,12,15,18-tetraoxa-6,22-diazaoctacosan-28-yl)carbamoyl)-2 nitrosobenzoate; $O_2^{\bullet -}$: superoxide; $ONOO^-$: peroxynitrite; PBS: phosphate buffer saline; PEG: polyethylene glycol; pHBECs: primary human bronchial epithelial cells; pro-Cat: procathepsin; ROS: reactive oxygen species; RNS: reactive nitrogen species; SIN-1: 3-morpholinosydnonimine; TNF: tumor necrosis factor; Z: benzyloxycarbonyl.

**Introduction:**

Chronic obstructive pulmonary disease (COPD) is a foremost cause of death and morbidity worldwide [1]. Although the prevalence of the disease is increasing, no therapies are currently available. COPD is a heterogeneous disease that encompasses emphysema, chronic bronchitis, small airway obstruction and/or fibrosis, and is associated to mucus hyper secretion. The progressive and irreversible airflow obstruction is combined with an abnormal inflammatory response of the lungs punctuated by exacerbation episodes [2]. The mechanistic basis underlying COPD is complex and involves oxidative stress (oxidant/antioxidant imbalance), protease/antiprotease imbalance, but also environmental offense, host genetic and epigenetic factors [3]. Cigarette smoking is the major cause of COPD, by increasing the epithelium permeability and the recruitment of inflammatory cells that contribute to chronic airway inflammation and pathological lung tissue remodeling. Moreover, cigarette smoke (CS) increases directly the burden of oxidants in the respiratory tract. Among CS constituents, numerous oxidant chemicals were identified, such as semiquinones and aldehydes (e.g. acrolein, formaldehyde). CS is also a prominent source of reactive oxygen species (ROS) and reactive nitrogen species (RNS). Both species initiate protein oxidation, participate in the alteration of the extracellular matrix and may induce apoptosis [4]. ROS and RNS include superoxide ($O_2^{\bullet -}$), hydrogen peroxide ($H_2O_2$), nitric oxide (NO), or peroxynitrates. NO react with $O_2^{\bullet -}$ to form peroxynitrite ($ONOO^-$), a highly potent oxidizing molecule, which in turn can react with thiols [5].

Proteases are key components of regulatory mechanisms, through irreversible cleavage of substrates resulting in their activation, inactivation, or modulation of function [6,7]. For a long time, matrix metalloproteinases (MMPs) and serine proteases (e.g. neutrophil elastase, membrane-anchored matriptase) are closely associated with the development of emphysema. Among matrix metalloproteinases, MMP-12 plays a pivotal role in the pathology of COPD by directly and indirectly enhancing the elastinolytic and proteolytic potential of neutrophils and macrophages [8]. Recently, findings evidenced the emerging roles of ADAM proteases (A Disintegrin And Metalloproteinases) during COPD [9]; e.g. overexpression of ADAM10 in lung epithelium causes the development of experimental emphysema [10]. Also, pro-inflammatory neutrophil elastase is thought to contribute to COPD pathogenesis [11], and an imbalance between neutrophil-derived proteases (neutrophil elastase, cathepsin G, and proteinase 3) and their extracellular inhibitors is considered an important pathogenic mechanism that is associated to the onset of emphysema [12]. Beside these well documented proteases, human cysteine cathepsins (i.e. cathepsins B, C, F, H, K, L, O, S, V, W and X) take part in diverse biological processes and

participate in pulmonary homeostasis, although their exact functions in lung need to be clarified [13–16]. Cathepsins are primarily lysosomal/endosomal proteases that are produced by a broad variety of cell types including fibroblasts, macrophages and epithelial cells [17–19]. Nevertheless, they are also found in the pericellular environment as secreted soluble enzymes or associated with cell surfaces [20]. Lung cysteine cathepsins are involved in the degradation/recycling of extracellular matrix and basement membrane constituents as well antimicrobial peptides [9,21,22]. Their dysregulation contributes to lung illnesses such as emphysema, chronic bronchitis, idiopathic pulmonary fibrosis, cystic fibrosis, and asthma [7,21,23]. Accordingly, we identified cysteine cathepsins in bronchoalveolar lavage fluids (BALFs) and sputa of patients with acute inflammations, cystic fibrosis and silicosis [24–26]. Extracellular cathepsin S (CatS) remains stable at neutral pH contrary to other related cathepsins that are rapidly inactivated [23]. Cigarette smoke extract (CSE) enhances production of IL-18 (an IFN-γ inducing cytokine), which subsequently stimulates the expression of CatS in lung macrophages [27]. Additionally, IL-13, IFN-γ, IL-1 and TNF-α trigger CatS expression in murine models of induced asthma and COPD diseases [28–30]. Recently, we demonstrated that active CatS is overexpressed in the lung of current smokers compared to never-smokers; moreover CSE-exposed primary human bronchial epithelial cells (pHBECs) expressed and secreted in a dose dependent manner CatS that remains partly active despite presence of oxidants [31]. Accordingly, given its compelling elastinolytic activity, overexpression of active CatS may be harmful to lung homeostasis and plays a deleterious role in the pathophysiology of COPD [32]. Thus, pharmacological inhibition of CatS could be a valuable therapeutic option to reduce the severity of emphysema [23,33–35].

Cysteine is a key amino acid of enzyme function/regulation that may exist at different oxidative states (see for review: [36–39]). The sulfhydryl group of the conserved thiolate-imidazolium pair (Cys25, His159) of the active site of cathepsins acts as a highly reactive nucleophile in a combination of covalent and acid-base catalysis [40]. Cys25 (papain numbering) was also reported to be highly sensitive to oxidations and chemical modifications, consistently to its low acidic pKa (pKa ~ 4/4.5) [41]. Hence, lysosomal cathepsins B, K and L were inhibited by peroxides [42–44] and analogous observations were reported for caspases [45]. Nevertheless, the resistance of secreted CatS to oxidative stress induced by cigarette smoke exposure remains a puzzling question, which has never been addressed at our knowledge. Thus we decided to decipher *in vitro* CatS resistance to CSE by selecting four predominant and representative chemicals (among numerous oxidants found in a cigarette puff) to provide some rational bases to CatS stability : hydrogen peroxide ($H_2O_2$), formaldehyde (FA), acrolein (a.k.a propenal, a Michael acceptor) and peroxynitrite ($ONOO^-$; using SIN-1 as the peroxynitrite donor), respectively.

## Material and methods:

### Chemicals and oxidants:

Schiff's reagent, L-3-carboxy-trans-2, 3-epoxy-propionyl-leucylamide-(4-guanido)-butane (E-64), ethylene diamine tetra acetic acid (EDTA), polyethylene glycol lauryl ether (Brij35), dithiothreitol (DTT), glutathione (reduced form, GSH) and N-acetyl cysteine were obtained from Sigma-Aldrich (Saint Quentin Fallavier, France). Benzyloxy-carbonyl-Phe-Arg-7-amino-4-methyl coumarin (Z-FR-AMC) was purchased from Bachem (Bubendorf, Switzerland). SIN-1 (3-morpholinosydnonimine, HCl) was supplied by Calbiochem (Merck Millipore SAS, Guyancourt, France). Hydrogen peroxide ($H_2O_2$), formaldehyde (FA), and acrolein (prop-2-enal) were supplied by Sigma-Aldrich. The OxyBlot protein oxidation detection kit was provided by Calbiochem.

### Enzymes:

Recombinant human procathepsin S was expressed in *Escherichia coli* and purified as previously described [46]. Processing of pro-CatS to mature active CatS was conducted in 0.1 M sodium acetate buffer pH 4.0, containing 2 mM DTT, 1 mM EDTA, 0.01% Brij 35, for 5 h at 26°C [47]. The activity buffer of CatS was 0.1 M sodium acetate buffer pH 5.5, containing 2 mM DTT, 1 mM EDTA, 0.01% Brij 35. Cat S activity was recorded using as substrate Z-FR-AMC ($\lambda ex$ = 350 nm, $\lambda em$ = 460 nm). The fluorescence release was monitored using a Spectramax Gemini spectrofluorometer (Molecular Devices, Saint Grégoire, France). The active concentration of CatS was determined by titration with E-64. Catalase from bovine liver was supplied by Sigma-Aldrich.

### Probes:

Biotinyl-$(PEG)_2$-Ahx-Leu-Val-Gly-DMK, a cystatin-derived activity-based probe, was synthetized as reported elsewhere [48]. The sulfenic acid probe, biotin-1,3-cyclopentanedione (BP1) was purchased from Kerafast, Inc. (Boston, MA, USA) [49]. The NO-Bio sulfinic acid probe that consists of a 2-nitroso terephthalic acid warhead coupled to a biotin tag by a PEG spacer was supplied by Kerafast [50]. The extravidin-peroxydase conjugate came from Sigma-Aldrich.

### Preparation of cigarette smoke extracts (CSE):

CSE was prepared as previously described [31,51]. Mainstream smoke of three filter Research-grade cigarettes (reference: 3R4F; Kentucky Tobacco Research and Development

Center at the University of Kentucky, Lexington, KY) was bubbled in 0.1 M sodium acetate buffer, pH 5.5 (50 mL) or in 100 mM HEPES buffer, pH 7.4 (50 mL) in a closed environment (average burning time/cigarette: ~8 min). The obtained solution was considered as 100% CSE, and was aliquoted and stored at -80°C. CSE preparation was standardized by measuring the absorbance of polycyclic compounds (quinic acid and nicotine) (λ=320 nm; Cary 100 spectrophotometer, Agilent Technologies, Les Ulis, France). The oxidative potential of CSE was determined by the redox conversion of reduced (non-fluorescent) dihydro-rhodamine-123 to oxidized (fluorescent) rhodamine-123 (Sigma-Aldrich), as previously detailed [31]. Released fluorescence was quantified using a calibration curve of rhodamine-123 (0 to 200 nM) (Cary Eclipse spectrofluorometer, Agilent Technologies, Les Ulis, France; λex = 490 nm, λem = 530 nm). For information, no difference in the redox conversion of dihydro-rhodamine-123 to oxidized rhodamine-123 was measured between aliquoted samples of CSE stored at -80°C and freshly prepared CSE.

**Inactivation of elastinolytic activity of cathepsin S:**

The elastinolytic activity of CatS (1nM) was recorded using DQ-elastin (25 µg/mL, Thermo Fisher Scientific, Illkirch-Graffenstaden, France) as a fluorogenic substrate (λex = 490 nm, λem = 515 nm) in the presence of increasing amounts of CSE (0-10%) during 30 min at 37°C in 0.1 M sodium acetate buffer pH 5.5, containing 1 mM EDTA, 0.01% Brij 35 and 15 µM DTT (Cary Eclipse spectrofluorometer, Agilent Technologies). Assay were repeated in 0.1 M HEPES buffer pH 7.4, containing 1 mM EDTA, 0.01% Brij 35 and 15 µM DTT. Results are representative of three independent experiments, each performed in triplicate.

**Inactivation of cathepsin S by CSE or by major CS oxidants:**

**Kinetic assays:** The activity of CatS (1 nM) was measured at 37°C in 0.1 M sodium acetate buffer pH 5.5, containing 1 mM EDTA, 0.01% Brij 35 and 15 µM DTT with increasing amounts of CSE (0-40%) in 96-well microplates (Nunc, Thermo Fisher Scientific), using Z-FR-AMC (20 µM) as substrate (λex = 350 nm, λem = 460 nm; Spectramax Gemini spectrofluorometer). The same assay was performed in 0.1 M HEPES buffer pH 7.4, containing 1 mM EDTA, 0.01% Brij 35 and 15 µM DTT. Alternatively, kinetic analysis of CatS inactivation was performed in the presence of CS oxidants, $H_2O_2$ (0-250 µM), acrolein (0-300 µM), FA (0-1000 µM), and $ONOO^-$ (0-1000 µM), respectively. SIN-1 (range: 0-4000 µM) was used as the parent peroxynitrite donor in order to generate an estimated 0-1000 µM concentration of $ONOO^-$ (i.e. four times lower than SIN-1) as previously reported by Rodrigues-Lima and collaborators

[52]. Assays were performed under pseudo-first-order conditions. Progress curves were fitted by non-linear regression analysis. Experimental data best matched with the first-order equation: P = L. [1-exp (-$k_{obs}$.t)], where P represents the product formation at time t, L represents the limiting rate and $k_{obs}$ is the apparent first-order rate constant (Enzfitter software; Biosoft, Cambridge, UK). Values of $k_{inact}$ (the first-order rate constant of enzyme inactivation) were further calculated using the equation $k_{obs} = k_{inact} / (1 + S_0/K_m)$ as described elsewhere [53], where $K_m$ is the Michaelis constant of CatS for Z-FR-AMC ($K_m$ = 22 µM, [54] ; $S_0$ = 20 µM). Plots of $k_{inact}$ values *vs* oxidant concentrations ([I]) gave a linear fit. The slope of plots corresponded to the second-order rate constant $k_{inact}$/[I] (n=3, three independent experiments).

**Endpoint assays:** CatS (1 nM) was incubated 20 min at 37°C with increasing amounts of CSE (0-40%), $H_2O_2$ (0-300 µM), $ONOO^-$ (0-625 µM), acrolein (0-300 µM) or FA (0-1000 µM) respectively, in 0.1 M sodium acetate buffer pH 5.5, containing 1 mM EDTA, 0.01% Brij 35 and 15 µM DTT. Residual activity was measured using the substrate Z-Phe-Arg-AMC (20 µM) (Spectramax Gemini spectrofluorometer; λex = 350 nm, λem = 460 nm). Alternatively, experiments were also performed in 0.1 M HEPES buffer pH 7.4, containing 1 mM EDTA, 0.01% Brij 35 and 15 µM DTT, using CSE (0-40%), $H_2O_2$ (0-1000 µM), $ONOO^-$ (0-500 µM), acrolein (0-100 µM) or FA (0-1000 µM). Three independent assays were done in triplicate.

**Maturation of procathepsin S in presence of oxidants or CSE:** Autoprocessing of pro-CatS (1 µg) was performed in 0.1 M sodium acetate buffer pH 4.0, 15 µM DTT, 1 mM EDTA, 0.01% Brij 35 for 0-12 h at 26°C in the presence of increasing concentration of oxidants (0-1000 µM) or in presence of CSE (0-40%). Samples were then diluted in Laemmli buffer, boiled and subjected to a 15% SDS-PAGE under reducing conditions. Gels were stained with Coomassie Brilliant blue G-250. The same experiment was repeated except that samples were further incubated with a molar excess (1:200) of Biot-$(PEG)_2$-Ahx-LeuValGly-DMK [48]. After electrophoresis and transfer onto nitrocellulose membrane, samples were incubated with an extravidin-peroxydase conjugate (Sigma-Aldrich, 1:2500 in PBS 1X, BSA 3%, Tween20 0.1%), and visualized by chemiluminescence (ECL Plus Western blotting detection system; Amersham Biosciences, Buckinghamshire, UK) according to the manufacturer's instructions.

**Evaluation of the oxidation status of CatS by immunodetection of carbonyl groups:**

Protein carbonylation of CatS following incubation with $H_2O_2$ (0-300 µM) was assessed using the OxyBlot protein oxidation detection kit (Merck Millipore). Briefly, CatS (500 nM) was incubated with increasing amounts of $H_2O_2$ at 37°C in 0.1 M sodium acetate buffer pH 5.5, 15

µM DTT, 1 mM EDTA, 0.01% Brij 35 during 30 min before adding catalase (10 nM). Protein samples were further treated with a dinitrophenylhydrazine (DNPH) derivatization solution at room temperature for 15 min. DNPH-tagged CatS was submitted to a 15% SDS-PAGE and transferred onto a nitrocellulose membrane. Finally, DNPH-derivatized samples were incubated with a murine anti-DNP antibody (1:150), then a peroxydase-conjugated secondary antibody (1:300). The carbonylation level of CatS was revealed by ECL. The same experiment was performed in presence of CSE (0-40%).

**Reversibility of CatS activity:**

CatS (1 nM) was incubated for 20 min with increasing concentrations of $H_2O_2$ (0-200 µM). Then, DTT (2 mM) was added and the restored CatS activity was measured by monitoring fluorescence release using Z-FR-AMC (20 µM) as substrate (λex = 350 nm, λem = 460 nm; Cary eclipse spectrofluorometer, Agilent Technologies, France). The experiment was repeated in 0.1 M HEPES buffer pH 7.4, containing 1 mM EDTA, 0.01% Brij 35 and 15 µM DTT with increasing concentration of $H_2O_2$ (0-500 µM). Data were expressed as the mean ± SEM (n=3, three independent experiments). Alternatively, similar assays were performed with acrolein (0-300 µM at pH 5.5 and 0-30 µM at pH 7.4) and $ONOO^-$ (0-1250 µM), or in the presence of increasing amounts of CSE (0-40%) at both pH.

**Active site labeling of cathepsin S with a biotinylated activity-based probe:**

CatS (50 nM) was incubated during 30 min at 37°C in 0.1 M sodium acetate buffer pH 5.5, 15 µM DTT, 1 mM EDTA, and 0.01% Brij 35 with increasing amounts of oxidanst (0-1000 µM) and CSE (0-40%). The same experiment was performed in 0.1 M HEPES buffer pH 7.4, containing 15 µM DTT, 1 mM EDTA, and 0.01% Brij 35. Following incubation, the thiolate-directed probe, Biot-$(PEG)_2$-Ahx-LeuValGly-DMK (10 µM) was added during 15 min at 37°C [48]. Samples were separated on a 15% SDS-PAGE and transferred onto nitrocellulose membrane. Then samples were incubated with an extravidin-peroxydase conjugate and visualized by chemiluminescence (ECL Plus Western blotting detection system) as described above. The same experiment was completed using a constant amount of $H_2O_2$ (150 µM) and CSE (10%) during varying incubation times (0-420 min). Bands were quantified by densitometric analysis (ImageJ software, National Institutes of Health, Bethesda, MD, USA).

**Labeling of oxidized CatS by biotin-1,3-cyclopentanedione and by NO-Bio probes:**

CatS (50 nM) was incubated with $H_2O_2$ (150 µM) for 0 to 300 min, at 37°C in 0.1 M sodium acetate buffer pH 5.5, 15 µM DTT, 1 mM EDTA, 0.01% Brij 35. After removal of $H_2O_2$ by catalase (10 nM) during 5 min, samples were incubated in the presence of biotin-1,3-cyclopentanedione sulfenic acid (BP1) probe (10 µM) during 1 h at 37°C [49]. Alternatively, after removal of $H_2O_2$ by catalase, DTT (2 mM) was added to reduce reversible oxidized forms of CatS. After 30 min, recovered free thiols of the active site were trapped irreversibly by incubation with E-64 (100 µM) during 1 h at room temperature. Then the samples were incubated 1 h at 37°C with the NO-Bio sulfinic acid probe (10 µM), according to Carroll and coworkers [50]. Lastly reactions for both BP1- and NO-Bio- treated samples were stopped by addition of non-reducing Laemmli buffer and boiling. Samples were further separated on a 15% SDS-PAGE, transferred onto nitrocellulose membrane, incubated with an extravidin-peroxydase conjugate and revealed by chemiluminescence as reported earlier. Bands were quantified by densitometric analysis using the ImageJ software (National Institutes of Health, Bethesda, MD, USA).

**Circular dichroism:**

CD spectra of CatS (0.05 mg/ml) were obtained using a Jasco J-810 spectropolarimeter (Jasco France, Bouguenais, France) equipped with a Peltier thermostat system. The path length of the cell was 0.1 cm (Hellma, VWR International SAS, Fontenay-sous-Bois, France). Far UV measurements (200-250 nm) were performed at 37°C. CD spectra of CatS were recorded in 0.1 M sodium phosphate buffer pH 5.5 after 6 h of incubation with 40% CSE and $H_2O_2$ (1000 µM) respectively. A CD control assay was done in the absence of oxidants. Baseline recordings were performed before each experiment and subtracted to CatS spectra. Data acquisitions were made at 1 nm intervals with a dwell time of 1 s between 200 and 250 nm and averaged from three repeated scans. The observed ellipticity ($\theta_d$) was converted in mean residue ellipticity using the formula $\theta_{mr} = \theta_d \times (M / C \times l \times n_r)$, where $\theta_{mr}$ is the mean residue ellipticity (deg.cm$^2$/dmol), $\theta_d$ is the observed ellipticity (mdeg), M is molecular weight (g/mol), C is the concentration of CatS (g/L), l is the pathlength (cm) and $n_r$ is the number of residues. The aminoacid sequence of CatS was obtained from UniProtKB/Swiss-Prot (ID: P25774) and its secondary structure composition was calculated using "the Secondary Structure Server" (http://2struc.cryst.bbk.ac.uk/) [55]. The secondary structure content of CatS was assessed by deconvolution of the CD spectra using the "Spectra Manager" software (Jasco).

**Chemical stability of CS oxidants:**

**NMR studies:** Stability of acrolein over time was controlled by pre-incubating the molecule in 0.1 M sodium acetate buffer pH 4.0 or 0.1 M sodium acetate buffer pH 5.5 or 0.1 M phosphate buffer pH 7.4 for 1 h, before performing NMR analysis. Acrolein (50 µM) was added to deuterium oxide 99% solution ($D_2O$, 50 µL) to set up the spectrometer (final volume: 210 µL). The resulting solution was transferred to a 3mm NMR tubes (CortecNet, Paris, France). Measurements were performed on a Bruker AVANCE III 600MHZ spectrometer (Bruker Sadis, Wissembourg, France), operating at 14T, with a TCI cryoprobe head, equipped with a Z-gradient coil. NMR measurements were performed at 25°C. Standard $^1H$ NMR spectra were acquired using a "noesypr1d" pulse sequence (relaxation delay of 5 s, mixing time of 10 ms, 8 scans on 64K data points and a spectral width of 12 ppm). Water suppression was achieved by presaturation during the relaxation delay and mixing time (Bruker Sadis). Spectra were corrected for phase distortion and baseline correction. The same NMR experiment was repeated for SIN-1 (50 µM).

**Spectroscopic analysis:** FA (500 µM) was incubated (0-1 h, 37°C) in the three buffers used for the experiments. Schiff's reagent (a.k.a. fuchsin-sulphurous acid) was added at t=0 and t=1 h, respectively, according to the protocol provided by the supplier (Sigma-Aldrich). Stability of FA was deduced from its aldehyde content measured at λ=553 nm (Spectramax Gemini spectrophotometer). The stability of $H_2O_2$ (1000 µM) in the different buffers (0-1 h, 37°C) was determined by monitoring its specific absorbance at 250 nm (Cary 100 UV visible spectrophotometer) [56].

**Statistical analysis:** Data are expressed as means ± standard error of the mean (SEM). Statistical significance between the different values was analyzed by nonparametric Mann-Whitney U test and group comparisons were performed with nonparametric Kruskal-Wallis test. Statistical analysis was performed using GraphPad Prism 6.01 (GraphPad Software, San Diego, CA). Differences at $p < 0.05$ were considered significant.

**Results & Discussion:**

**Inactivation of the elastinolytic activity of CatS:**

Contrary to other cysteine cathepsins that are rapidly inactivated at neutral pH, CatS remains stable and active extracellularly [23]. Earlier studies have demonstrated the key role of CatS in the extensive degradation of elastin fibers, supporting that it contributes to ECM remodeling associated to lung inflammations during COPD and emphysema [32]. In a recent report we demonstrated that CatS expression is significantly increased in the lung tissue of current smokers and correlates positively with pack-years of cigarette smoking [31]. Moreover, exposure of primary human bronchial epithelial cells to CSE induces CatS release via the activation of P2X7 receptors, which in turns drives p38 MAPK pathway [31]. Thus, we first tested the ability of CatS to degrade DQ-elastin in the presence of CSE (0-40%) at both pH 7.4, mimicking the pH of the extracellular medium and at pH 5.5 (Figure 1a). The elastinolytic activity of CSE exposed-CatS was partly impaired in a dose-dependent manner, but no significant difference was observed between both acidic and neutral pH. However, this CSE-dependent inactivation remained weak since most of the proteolytic activity (>70%) was preserved in the presence of 40% CSE. Then, CatS was incubated in the presence of CSE, before measurements of the residual peptidase activity. Endpoint assays indicated that CSE (0-10%) incompletely impaired its peptidase activity at pH 5.5, and had only a faint effect at pH 7.4 (Figure 1b). Nevertheless, higher (i.e. supra-physiological) levels of CSE led to CatS inactivation at both neutral and acidic pH. These data support that CatS exhibits a worthy resistance to inactivation by cigarette smoke at neutral pH, thus allowing it to maintain its elastinolytic activity in the presence of oxidizing agents. Accordingly, it should be noticed that the mucosal pH of inflamed airways of smokers is neutral/weakly basic (circa 7.2-7.3), unlike normal airway surface liquid (slightly acidic pH averaging 6.6 in healthy airway mucosa) (see for review: [57]). Also these findings endorse previous reports, which pointed that extracellular cysteine cathepsins were still enzymatically active in BALFs from patients exposed to oxidative stress and suffering of acute lung injury and infiltrative inflammatory disorders [24]. However, it has to be kept in mind that CSE correspond to a complex mixture of buffer-miscible chemicals in solution, while cigarette smoke, which is a dynamic aerosol embracing droplets of condensed liquids (particles or tar) suspended in a mixture of volatile/semi-volatile compounds (gas-phase smoke) encompasses distinctive chemical and physical properties [58]. Given these differences, we cannot exclude unlike effects of CSE and cigarette smoke on CatS activity.

**Kinetics of inactivation by major CS oxidants:**

According to this pivotal result, we decided to decipher CatS resistance to major and representative CSE oxidants: hydrogen peroxide ($H_2O_2$), acrolein, formaldehyde (FA) and peroxynitrite ($ONOO^-$). First, we assessed the pH-dependent stability of the four chemicals in order to circumvent any bias associated with a possible damage of the oxidants, depending on the nature of the buffers used. Analyses of the samples by spectroscopy or by 1D NMR showed that molecules were chemically stable and that their molecular integrity was not affected by the different buffers (experimental pH range: 4.0-7.4) (Supplementary figure 1). Then, CatS was incubated for 20 min at both pH 5.5 and pH 7.4 in the presence of $H_2O_2$, acrolein, FA, and $ONOO^-$, respectively, before measurements of the residual peptidase activity. $H_2O_2$ inactivated more efficiently CatS at pH 5.5 (50% of the peptidase activity was inhibited by 95 µM $H_2O_2$) than at pH 7.4 (50% of the activity was inhibited by 280 µM $H_2O_2$) (Figure 2a), conversely to acrolein (100 µM (pH5.5) vs 30 µM (pH7.4)), which is a highly reactive electrophile (Michael acceptor) (Figure 2b). $ONOO^-$ inhibited CatS similarly at both acidic (50% of inactivation by 100 µM $ONOO^-$) and neutral pH (50% of inactivation by 145 µM $ONOO^-$) (Figure 2c). Although both acrolein and FA encompass an aldehyde function, formaldehyde was poorly efficient toward CatS since 50% of the peptidase activity was preserved in the presence of 650 µM FA (pH5.5) and 700 µM FA (pH7.4) (Figure 2d). Time-dependent analyses of CatS inactivation were further conducted in the presence of increasing concentrations of oxidants (see: Supplementary figure 2). Apparent first-order rate constant ($k_{obs}$) and first-order rate constant ($k_{inact}$) were determined by non-linear regression analysis. Interestingly, plots of $k_{inact}$ values *vs* oxidant concentrations ([I]) fitted linearly, suggesting that CatS inactivation may obey a single-step mechanism. Second-order rate constants $k_{inact}/[I]$ were obtained by plotting $k_{inact}$ values *vs* oxidant concentrations ([I]) (Table 1). Quantitative analysis of the second-order rate constant values confirmed that FA is a weak oxidant of CatS. $ONOO^-$ exhibited similar $k_{inact}/[I]$ values at both pH 5.5 and pH 7.4. On the other hand, $H_2O_2$ inactivated more effectively CatS at pH 5.5, while acrolein was more potent at neutral pH. Kinetics results correlated with those monitored during the inactivation of elastinolytic activity (Figure 1a), sustaining that CatS may have deleterious properties during emphysema, given its high stability against chemical agents contained in cigarette smoke.

For comparison, experiments of inactivation by major chemicals from cigarette smoke were repeated in the presence of cathepsin K. Of note, CatK being rapidly inactivated at neutral pH [59], the trials were carried out at pH 5.5. No significant difference in CatK activity was observed in the absence or presence of CSE ($p>0.05$) (Supplementary figure 3). Then the

peptidase activity of CatK was measured following incubation in the presence of formaldehyde, hydrogen peroxide, peroxynitrite and acrolein, respectively (endpoint assays). Data showed that CatK is more sensitive than CatS to inactivation by hydrogen peroxide and formaldehyde. Conversely peroxynitrite inactivated CatS more efficiently than CatK, while the profile of inactivation by acrolein was comparable for both enzymes. These dissimilar results, which depended most probably on the nature of the chemical used, suggest that subtle differences in susceptibility to oxidation exist between papain-related cathepsins, despite a strong structural similarity and similar enzymatic specificities [18].

**Time- and dose-dependent oxidation of Cys25:**

CatS was incubated with $H_2O_2$ (150 µM) or CSE (10%), before adding the activity-based probe Biot-$(PEG)_2$-Ahx-LeuValGly-DMK to tag specifically the nucleophilic Cys25 of the active site [48]. We observed a time-dependent decrease of labeling of the thiolate group at pH 5.5 (Figure 3a). The signal loss was slower at pH 7.4 (Figure 3b) in agreement with kinetics data, endorsing that CatS is more sensitive to $H_2O_2$ inactivation at acidic pH. In the presence of 10% CSE, we observed an analogous time-dependent labeling profile with a higher stability of CatS at neutral pH, again matching kinetic analysis of inactivation. Then, CatS was incubated for 30 min at both pH 5.5 and pH 7.4 in the presence of increasing amounts (0-1000 µM) of $H_2O_2$, acrolein, $ONOO^-$ and FA, as well CSE (0-40%) (Figure 3 c-d). The slight variation of CatS labeling by Biot-$(PEG)_2$-Ahx-LeuValGly-DMK, following incubation with FA, confirmed that this chemical is a poor inactivator of CatS at both pH. Incubations with $H_2O_2$, acrolein, $ONOO^-$ and CSE led to a dose- and pH-dependent decrease of active Cys25 labeling (Figure 3 c-d), and corroborated kinetics data (Figure 1b, Figure 2). Additionally, the carbonylation of protein side chains is a valuable marker of oxidative stress that is frequently observed in acute and chronic diseases [60]. Beside oxidation of Cys25, a dose-dependent increase of carbonylation was observed in the presence of $H_2O_2$ and CSE (Figure 4 a-b). Further investigations by CD spectroscopy were performed (Figure 4 c-d). Far UV CD spectra of CatS were analyzed in the absence (experimental values, helix %: 32.8 ±1, beta sheet %: 24±2, others %: 45±3) or in the presence of $H_2O_2$ (experimental values, helix %: 32.2 ±3, beta sheet %: 26.5±4, others %: 42.3±6). The lack of significant modifications of CD spectra resulting from treatment by $H_2O_2$ (1000 µM) supported that both oxidation of Cys25 and formation of carbonyl derivatives had no substantial consequences on CatS secondary structure (helix %: 31, beta sheet %: 24, others %: 45), as deduced from its three-dimensional structure (http://2struc.cryst.bbk.ac.uk/; [55]). Likewise, we obtained similar results after treatment of CatS by 10% CSE (experimental values, helix %: 30.2

±5, beta sheet %: 24.2±8, others %: 45.7±10). Despite a wide CSE-dependent carbonylation, no obvious changes in the structural organization were observed, strengthening the scarce resistance of CatS to oxidative stress. CD data consolidate the notion that CatS could remain active and participates in remodeling of elastin fibers during COPD [31,32], regardless of the oxidation status of its peptide backbone.

**Reversibility of CatS inactivation:**

Following incubation at both pH 5.5 and pH 7.4 in the presence of CSE, $H_2O_2$, acrolein and $ONOO^-$, the ability of a reducing agent to restore CatS activity was evaluated. Assays were not performed with FA, given its low efficiency against CatS. Following incubation with $H_2O_2$, a partial recovery of CatS peptidase activity (expressed as mean ± SEM) was observed at pH 5.5 (24 % ± 2 %) and pH 7.4 (20 % ± 3 %) after addition of DTT (2 mM) (Figure 5a) (non-significant differences between different doses at both pH, non-parametric Kruskal-Wallis test). The rescue of activity CatS did not depend on $H_2O_2$ concentration. Accordingly a close restoration of CatK activity (~1/3 of the initial peptidase activity), corresponding to the formation of a DTT-reversible sulfenic acid (figure 5b), was reported [42]. This suggests that it may correspond to a fairly general mechanism for cysteine cathepsins. Nevertheless, in the present study, we failed to identify the diverse oxidized forms of Cys25-containing tryptic peptides by mass spectrometry analysis as reported above [42]. Following inactivation by 10% CSE at pH 5.5, we observed a nearby reversibility of CatS activity (31 % ± 5) by DTT. Likewise, CatS activity was restored in a similar manner in the presence of glutathione (reduced form, GSH) and N-acetyl cysteine (pH 5.5, 19% ± 4; 22% ± 4, respectively). Conversely DTT did not significantly fix up CatS activity after reaction with acrolein. This result was expected since acrolein was known to react with thiolate by forming a highly stable Michael addition adduct (Figure 5c). No concentration-dependent effect was observed, as already reported in the presence of $H_2O_2$. On the other hand, a different situation was observed in the presence of $ONOO^-$ that inhibited similarly CatS at both pH 5.5 ($k_{inact}/[I] = 4.0 \pm 1.6\ M^{-1}.\ s^{-1}$) and pH 7.4 ($k_{inact}/[I] = 4.9 \pm 0.8\ M^{-1}.\ s^{-1}$) (Table I). In the presence of an elevated concentration (1250 µM) of peroxynitrite, only ~8-10 % of the initial hydrolysis rate was regained (Figure 5a). This results supported that high concentrations of $ONOO^-$ inactivated irreversibly CatS as demonstrated for other peroxynitrite-sensitive enzymes [61–65]. As suggested previously, this inactivation could result from the oxidation of the active site sulfhydryl group to irreversible sulfinic and/or sulfonic acids [61–63]. On the other hand *circa* 36-42 % of CatS activity was restored by DTT, following treatment by lower $ONOO^-$ concentration (125 µM). As reported elsewhere, these data sustain that the chemical reaction of

$ONOO^-$ with Cys25 of CatS may partly lead to the formation of a reducible DTT-sensitive sulfenic acid or S-nitrosothiol (Figure 5d) [63,64]. Likewise, Väänänen and colleagues proposed that the inactivation of thiol-dependent proteases by nitric oxide-related species could correspond to a protective mechanism besides the known irreversible oxidation by some harmful oxidants (e.g. hypochlorous acid) [62].

**Labeling of CatS by redox sensing probes:**

This study was carried out following peroxide treatment (150 µM $H_2O_2$; 0-300 min) and removal of $H_2O_2$ by an enzymatic treatment (10 nM catalase). The oxidation status of the active site thiol of CatS was investigated by using both sulfenic and sulfinic redox sensing probes [49,50], as described in the experimental section. Interestingly untreated CatS (t=0) was labeled by both biotin-1,3-cyclopentanedione (BP1, sulfenic acid probe) and NO-Bio (sulfinic acid probe) (Figure 6a; see Figures 6b and 6c for trap mechanisms). This observation is consistent with the result of the E-64 titration, i.e. 40% of active (reduced form) CatS, which supports that a large amount of CatS has undergone oxidation during the preparative (purification and activation) steps [47]. Present results obtained using both BP1 and NO-Bio redox sensing probes support that catalytically active CatS was oxidized sequentially, i.e. via the formation of a reversible sulfenic acid (0-60 min) before a slower conversion to irreversible sulfinic acid, as suggested by the densitometric analysis of the BP1/NO-Bio ratio over time (Figure 6a). We did not evaluate the level of sulfonic acid due to the lack of an available and specific redox sensing probe. Nevertheless, the delayed increase of sulfinic acid could provide a mechanistic rational to the transitory stability of active CatS in the presence of $H_2O_2$. One could hypothesize that such sequential reaction may correspond to a transient protective machinery [44].

**Time- and dose-dependent inactivation of pro-CatS maturation by CS oxidants:**

Procathepsins represent an *in vivo* activatable reservoir of mature enzymes (for review: [21]). Such activation may have important physiological consequences because zymogens were often found secreted in various pathological conditions, including lung inflammations [24,26]. Accordingly, we analyzed the auto-processing of recombinant procathepsin S under *in vitro* conditions with increasing concentrations of CSE (0-40%) and oxidants (0-1000 µM). In the absence of treatment (Figure 7a, lane 2) pro-CatS was fully processed with the exception of a faint band of the intermediate processing form (*circa* 2/3 kDa higher molecular weight than mature form), corresponding to the mixture of two intermediate species (cleavage at both Ser76p-Ser77p and Met72p-Ser73p positions; CatS prosegment numbering) [66]. $H_2O_2$ inhibited in a dose-

dependent manner the maturation of pro-CatS. The activity-based probe Biot-$(PEG)_2$-Ahx-LeuValGly-DMK labelled mature CatS, but also its zymogen and the intermediate form, depending on $H_2O_2$ amount (Figure 7a). Remarkably, even after 12h incubation with $H_2O_2$ (1000 µM), the CatS proform still reacted with Biot-$(PEG)_2$-Ahx-LeuValGly-DMK, indicating that pro-CatS is catalytically active. Present data are in agreement with a previous report that demonstrated that pro-CatB, in addition to mature CatB, could react with an activity-based probe [67]. Also, acrolein inhibited pro-CatS maturation. However, the inhibitory profile was distinctive to that observed with $H_2O_2$, since the initial step of conversion of pro-CatS to the intermediate processing form still occurred as shown by Coomassie staining (Figure 7b), while a dose-dependent decrease in labeling by Biot-$(PEG)_2$-Ahx-LeuValGly-DMK was observed. On the other hand, $ONOO^-$ did not impair activation of pro-CatS to mature CatS (Figure 7c). Yet there was a significant decrease in CatS active site-labeling, which validated that mature CatS was inhibited by $ONOO^-$ following pro-CatS autoprocessing. FA did not prevent the maturation and activation of pro-CatS (Figure 7d). Finally, CSE exhibited a similar ineffectiveness (Figure 7e). According to cathepsin proforms represent a proteolytic reservoir (see for reviews: [21,68]), present results suggest that pro-CatS is still activable in the presence of cigarette smoke; subsequently, the autocatalytic maturation of pro-CatS could enhance the elastinolytic potential of active CatS despite a detrimental oxidative environment (Oxidative stress index (OSI) of 0.94±0.2 for smokers with COPD *vs* 0.59±0.1 for non-smokers) [31].

In overall, this study provided some mechanistic and molecular clues that may help to a better awareness of the contribution of active CatS to the pathophysiology of emphysema, via its unexpected resistance to CSE as well to representative CSE oxidants. Taken together the still unmet need for effective therapies for patients with emphysema and recent studies on CatS [31,32], a better understanding of the burst of CatS activation during cigarette smoke exposure is an essential step. Moreover, drug candidates that encompass both protease inhibition properties and antioxidant potential could therefore be considered promising therapeutics in the management of lung destruction in high-risk smokers.

**Acknowledgements:**

We are grateful to Prof. M-C. Viaud-Massuard (Molecular and Therapeutic Innovation (GICC), University of Tours, Faculty of Pharmaceutical Sciences, Tours, France) for comments. Dr M. Wartenberg was a recipient of a doctoral grant from the Région Centre-Val de Loire, France. Dr P-M. Andrault was a recipient of a doctoral grant from INSERM-Région Centre-Val de Loire, France. P. Bigot holds a doctoral fellowship from MESRI (Ministère de l'Enseignement Supérieur, de la Recherche et de l'Innovation, France). This work was supported by the Région Centre-Val de Loire, France (BPCO-Lyse project: # 201500103986). We acknowledge the Institut National de la Santé et de la Recherche Médicale (INSERM) for institutional fundings. These agencies played no role in study design, data collection and analysis, the decision to publish or preparation of the manuscript.

**Author contributions:** MW and GL designed research and planned studies. MW, P-MA, AS, PB and LN-D performed experiments. MW, FL and GL analyzed data. LN-D considered NMR data. MW prepared the figures. GL wrote the paper. MW, P-MA, AS, LN-D and FL revised the paper. All authors approved the final version of the manuscript.

**Competing Interests:** The authors declare no competing interest.

**Legend to Figures**

**Figure 1: Inactivation of elastinolytic and peptidase activity of cathepsin S by CSE.**

(a) The elastinolytic activity of CatS (1 nM) was recorded using DQ-elastin (25 µg/ml) as fluorogenic substrate (excitation wavelength: 490 nm; emission wavelength: 515 nm) in presence of increasing concentrations of CSE (0-40 %) during 30 min (37°C) in 0.1 M HEPES buffer pH 7.4, containing 1 mM EDTA, 0.01% Brij 35 and 15 µM DTT (white) and in 0.1 M sodium acetate buffer pH 5.5, containing 1 mM EDTA, 0.01% Brij 35 and 15 µM DTT (black). Slopes (release of fluorescence) were calculated and data were normalized relative to control without treatment (mean values expressed as %, n=3). (b) CatS (1 nM) was incubated for 20 min at 37°C at both pH 5.5 (●) and pH 7.4 (○) with increasing amounts of CSE (0-40%). The residual peptidase activity was monitored using Z-Phe-Arg-AMC (20 µM) ($\lambda_{ex}$ = 350 nm, $\lambda_{em}$ = 460 nm). Three independent assays were done in triplicate. Data are represented as the percentage of activity compared to untreated CatS (mean ± SEM, n=3). Statistical analyses were performed using Mann-Whitney U test and values were compared to control without oxidants (*: $p < 0.05$).

**Figure 2: Endpoint assay of cathepsin S in presence of oxidants.**

CatS (1 nM) was incubated for 20 min at 37°C in 0.1 M sodium acetate buffer pH 5.5, containing 1 mM EDTA, 0.01% Brij 35 and 15 µM DTT (●) or in 0.1 M HEPES buffer pH 7.4, containing 1 mM EDTA, 0.01% Brij 35 and 15 µM DTT (○) with increasing amounts of $H_2O_2$ (0-1000 µM), acrolein (0-300 µM), $ONOO^-$ (0-625 µM) and FA (0-1000 µM) respectively. (a) $H_2O_2$; (b) acrolein; (c) $ONOO^-$; (d) FA. The residual peptidase activity was monitored using Z-Phe-Arg-AMC (20 µM) ($\lambda_{ex}$ = 350 nm, $\lambda_{em}$ = 460 nm). Three independent assays were done in triplicate. Data are represented as the percentage of activity compared to untreated CatS (mean ± SEM, n=3).

**Figure 3: Time- and dose-dependent oxidation of Cys25.**

(a) CatS was incubated with CSE (10%) or $H_2O_2$ (150 µM) at pH 5.5 and pH 7.4 for 0-420 min. Biot-$(PEG)_2$-Ahx-LeuValGly-DMK, a biotinylated activity-based probe, was added for labeling of the nucleophilic Cys25 of the active site [48] as described in the experimental section. (b) Alternatively, CatS was incubated for 15 min at pH 5.5 and pH 7.4 in the presence of increasing amounts of CSE (0-40%), or $H_2O_2$, acrolein, $ONOO^-$ and FA (0-1000 µM). A representative experiment is shown (n=3). Bands were quantified by densitometric analysis (ImageJ software, National Institutes of Health, Bethesda, MD, USA). Data were normalized relative to control without oxidants and expressed as means ± SEM. Statistical analyses were performed using Mann-Whitney U test and values were compared to control without oxidants (*: $p < 0.05$).

**Figure 4: Structural consequences of CatS oxydation.**

CatS was incubated with (a) CSE (0-40%) or (b) $H_2O_2$ (0-300 µM), at pH 5.5 during 30 min as described before. Biot-$(PEG)_2$-Ahx-LeuValGly-DMK (i.e. ABP) was further added for active site labeling, while the carbonylation status of CatS was assessed by OxyBlot. A representative experiment is shown. Corresponding Far UV CD spectra (200-250 nm) of CatS were recorded in 0.1 M sodium phosphate buffer pH 5.5 after 6 h of incubation with (c) 40% CSE or (d) $H_2O_2$ (1000 µM). Baseline recordings were performed before each assay and subtracted to CatS spectra. Data (expressed as mean residue ellipticity) were averaged from three repeated

scans. The experimental secondary structure content of CatS was assessed by deconvolution of the CD spectra (Spectra manager software, Jasco) (mean ± SEM, n=3).

**Figure 5: DTT-dependent reversibility of CatS inactivation.**

(a) CatS (1 nM) was incubated for 20 minutes with CSE, $H_2O_2$, acrolein and $ONOO^-$. DTT (2 mM) was further added and CatS activity was measured using Z-FR-AMC (20 µM) as substrate. Recovery of the peptidase activity was expressed as the mean±SEM (n=3, three independent experiments) (100%: initial hydrolysis rate of untreated CatS). Diagrams of the oxidation mechanism of the thiol function in the presence of (b) $H_2O_2$, (c) acrolein (Michael acceptor), (d) $ONOO^-$. Black, bold type: major reaction pathway; gray, secondary reaction route.

**Figure 6: Labeling of sulfenic and sulfinic forms of CatS by redox sensing probes.**

CatS (50 nM) was incubated with $H_2O_2$ (150 µM) for 0-300 minutes at 37°C in 0.1 M sodium acetate buffer pH 5.5, 15 µM DTT, 1 mM EDTA, 0.01% Brij 35. After enzymatic removal of $H_2O_2$ by catalase (10 nM), samples were treated by biotin-1,3-cyclopentanedione sulfenic acid probe (BP1; 10 µM), consistent with [49]. Alternatively, samples were incubated with the NO-Bio sulfinic acid probe (10 µM), according to [50]. (a) After addition of non-reducing Laemmli buffer and boiling, samples were separated on a 15% SDS-PAGE, transferred onto nitrocellulose membrane, then incubated with an extravidin-peroxydase conjugate and revealed by chemiluminescence as reported earlier. The sulfenic acid /sulfinic acid ratio was obtained by densitometric analysis (ImageJ software). A representative sample is shown (n=3). Reaction mechanisms of redox sensing probes with active site thiol (Cys25): (b) sulfenic acid trapping by biotin-1,3-cyclopentanedione sulfenic acid probe, (c) sulfinic acid trapping by NO-Bio sulfinic acid probe.

**Figure 7: Inhibition of the automaturation of procathepsin S.**

Autoprocessing of procathepsin S (1 µg) was achieved in 0.1 M sodium acetate buffer pH 4.0, 15 µM DTT, 1 mM EDTA, 0.01% Brij 35 (12h, 26°C) in the presence of increasing concentrations (0-1000 µM) of: (a) $H_2O_2$; (b) acrolein; (c) $ONOO^-$; (d) FA. The same experiment was performed with increasing amounts of CSE (0-40%). Samples were separated on a 15% SDS-PAGE, and gels were stained with Coomassie Brilliant blue G-250 (top) (black arrow, pro-CatS; grey arrow, intermediate precursor; white arrow, mature CatS). Alternatively, samples were incubated with Biot-$(PEG)_2$-Ahx-LeuValGly-DMK (so called ABP). After 15% SDS-PAGE and transfer onto nitrocellulose membrane, samples were incubated with an extravidin-peroxydase conjugate and revealed by chemiluminescence (bottom). A representative sample is shown (n=3).

## References


[1] C.J. Murray, A.D. Lopez, Evidence-based health policy--lessons from the Global Burden of Disease Study, Science. 274 (1996) 740–743. https://doi.org/10.1126/science.274.5288.740.

[2] P.J. Barnes, Targeting cytokines to treat asthma and chronic obstructive pulmonary disease, Nat. Rev. Immunol. 18 (2018) 454–466. https://doi.org/10.1038/s41577-018-0006-6.

[3] B.M. Fischer, J.A. Voynow, A.J. Ghio, COPD: balancing oxidants and antioxidants, Int. J. Chron. Obstruct. Pulmon. Dis. 10 (2015) 261–276. https://doi.org/10.2147/COPD.S42414.

[4] S. Boukhenouna, M.A. Wilson, K. Bahmed, B. Kosmider, Reactive Oxygen Species in Chronic Obstructive Pulmonary Disease, Oxid. Med. Cell Longev. 2018 (2018). https://doi.org/10.1155/2018/5730395.

[5] K.G. Reddie, K.S. Carroll, Expanding the functional diversity of proteins through cysteine oxidation, Curr. Opin. Chem. Biol. 12 (2008) 746–754. https://doi.org/10.1016/j.cbpa.2008.07.028.

[6] L. Kramer, D. Turk, B. Turk, The Future of Cysteine Cathepsins in Disease Management, Trends Pharmacol. Sci. 38 (2017) 873–898. https://doi.org/10.1016/j.tips.2017.06.003.

[7] J. Reiser, B. Adair, T. Reinheckel, Specialized roles for cysteine cathepsins in health and disease, J. Clin. Invest. 120 (2010) 3421–3431. https://doi.org/10.1172/JCI42918.

[8] M.J. Banda, E.J. Clark, Z. Werb, Limited proteolysis by macrophage elastase inactivates human alpha 1-proteinase inhibitor, J. Exp. Med. 152 (1980) 1563–1570. https://doi.org/10.1084/jem.152.6.1563.

[9] C. Taggart, M.A. Mall, G. Lalmanach, D. Cataldo, A. Ludwig, S. Janciauskiene, N. Heath, S. Meiners, C.M. Overall, C. Schultz, B. Turk, K.S. Borensztajn, Protean proteases: at the cutting edge of lung diseases, Eur. Respir. J. 49 (2017). https://doi.org/10.1183/13993003.01200-2015.

[10] H. Saitoh, P.L. Leopold, B.-G. Harvey, T.P. O'Connor, S. Worgall, N.R. Hackett, R.G. Crystal, Emphysema mediated by lung overexpression of ADAM10, Clin. Transl. Sci. 2 (2009) 50–56. https://doi.org/10.1111/j.1752-8062.2008.00085.x.

[11] R.A. Sandhaus, G. Turino, Neutrophil elastase-mediated lung disease, COPD. 10 Suppl 1 (2013) 60–63. https://doi.org/10.3109/15412555.2013.764403.

[12] N. Guyot, J. Wartelle, L. Malleret, A.A. Todorov, G. Devouassoux, Y. Pacheco, D.E. Jenne, A. Belaaouaj, Unopposed cathepsin G, neutrophil elastase, and proteinase 3 cause severe lung damage and emphysema, Am. J. Pathol. 184 (2014) 2197–2210. https://doi.org/10.1016/j.ajpath.2014.04.015.

[13] A. Menou, J. Duitman, B. Crestani, The impaired proteases and anti-proteases balance in Idiopathic Pulmonary Fibrosis, Matrix Biol. 68–69 (2018) 382–403. https://doi.org/10.1016/j.matbio.2018.03.001.

[14] K.C. Pandey, S. De, P.K. Mishra, Role of Proteases in Chronic Obstructive Pulmonary Disease, Front. Pharmacol. 8 (2017) 512. https://doi.org/10.3389/fphar.2017.00512.

[15] P.J. Wolters, H.A. Chapman, Importance of lysosomal cysteine proteases in lung disease, Respir. Res. 1 (2000) 170–177. https://doi.org/10.1186/rr29.

[16] A. Saidi, M. Kasabova, L. Vanderlynden, M. Wartenberg, G.H. Kara-Ali, D. Marc, F. Lecaille, G. Lalmanach, Curcumin inhibits the TGF-β1-dependent differentiation of lung fibroblasts via PPARγ-driven upregulation of cathepsins B and L, Sci. Rep. 9 (2019) 491. https://doi.org/10.1038/s41598-018-36858-3.

[17] F. Lecaille, J. Kaleta, D. Brömme, Human and parasitic papain-like cysteine proteases: their role in physiology and pathology and recent developments in inhibitor design, Chem. Rev. 102 (2002) 4459–4488.

[18] V. Turk, V. Stoka, O. Vasiljeva, M. Renko, T. Sun, B. Turk, D. Turk, Cysteine cathepsins: from structure, function and regulation to new frontiers, Biochim. Biophys. Acta. 1824 (2012) 68–88. https://doi.org/10.1016/j.bbapap.2011.10.002.

[19] B. Korkmaz, G.H. Caughey, I. Chapple, F. Gauthier, J. Hirschfeld, D.E. Jenne, R. Kettritz, G. Lalmanach, A.-S. Lamort, C. Lauritzen, M. Łęgowska, A. Lesner, S. Marchand-Adam, S.J. McKaig, C. Moss, J. Pedersen, H. Roberts, A. Schreiber, S. Seren, N.S. Thakker, Therapeutic targeting of

cathepsin C: from pathophysiology to treatment, Pharmacol. Ther. (2018). https://doi.org/10.1016/j.pharmthera.2018.05.011.
[20] K. Brix, A. Dunkhorst, K. Mayer, S. Jordans, Cysteine cathepsins: cellular roadmap to different functions, Biochimie. 90 (2008) 194–207. https://doi.org/10.1016/j.biochi.2007.07.024.
[21] G. Lalmanach, A. Saidi, S. Marchand-Adam, F. Lecaille, M. Kasabova, Cysteine cathepsins and cystatins: from ancillary tasks to prominent status in lung diseases, Biol. Chem. 396 (2015) 111–130. https://doi.org/10.1515/hsz-2014-0210.
[22] F. Lecaille, G. Lalmanach, P.-M. Andrault, Antimicrobial proteins and peptides in human lung diseases: A friend and foe partnership with host proteases, Biochimie. 122 (2016) 151–168. https://doi.org/10.1016/j.biochi.2015.08.014.
[23] R.D.A. Wilkinson, R. Williams, C.J. Scott, R.E. Burden, Cathepsin S: therapeutic, diagnostic, and prognostic potential, Biol. Chem. 396 (2015) 867–882. https://doi.org/10.1515/hsz-2015-0114.
[24] C. Serveau-Avesque, M.F.-D. Martino, V. Hervé-Grépinet, E. Hazouard, F. Gauthier, E. Diot, G. Lalmanach, Active cathepsins B, H, K, L and S in human inflammatory bronchoalveolar lavage fluids, Biol. Cell. 98 (2006) 15–22. https://doi.org/10.1042/BC20040512.
[25] C. Perdereau, E. Godat, M.-C. Maurel, E. Hazouard, E. Diot, G. Lalmanach, Cysteine cathepsins in human silicotic bronchoalveolar lavage fluids, Biochim. Biophys. Acta. 1762 (2006) 351–356. https://doi.org/10.1016/j.bbadis.2005.10.005.
[26] C. Naudin, A. Joulin-Giet, G. Couetdic, P. Plésiat, A. Szymanska, E. Gorna, F. Gauthier, F. Kasprzykowski, F. Lecaille, G. Lalmanach, Human cysteine cathepsins are not reliable markers of infection by Pseudomonas aeruginosa in cystic fibrosis, PLoS One. 6 (2011) e25577. https://doi.org/10.1371/journal.pone.0025577.
[27] M.-J. Kang, R.J. Homer, A. Gallo, C.G. Lee, K.A. Crothers, S.J. Cho, C. Rochester, H. Cain, G. Chupp, H.J. Yoon, J.A. Elias, IL-18 is induced and IL-18 receptor alpha plays a critical role in the pathogenesis of cigarette smoke-induced pulmonary emphysema and inflammation, J. Immunol. 178 (2007) 1948–1959.
[28] K. Deschamps, W. Cromlish, S. Weicker, S. Lamontagne, S.L. Huszar, J.Y. Gauthier, J.S. Mudgett, A. Guimond, R. Romand, N. Frossard, M.D. Percival, D. Slipetz, C.M. Tan, Genetic and pharmacological evaluation of cathepsin s in a mouse model of asthma, Am. J. Respir. Cell Mol. Biol. 45 (2011) 81–87. https://doi.org/10.1165/rcmb.2009-0392OC.
[29] Z. Wang, T. Zheng, Z. Zhu, R.J. Homer, R.J. Riese, H.A. Chapman, S.D. Shapiro, J.A. Elias, Interferon gamma induction of pulmonary emphysema in the adult murine lung, J. Exp. Med. 192 (2000) 1587–1600.
[30] T. Zheng, Z. Zhu, Z. Wang, R.J. Homer, B. Ma, R.J. Riese, H.A. Chapman, S.D. Shapiro, J.A. Elias, Inducible targeting of IL-13 to the adult lung causes matrix metalloproteinase- and cathepsin-dependent emphysema, J. Clin. Invest. 106 (2000) 1081–1093. https://doi.org/10.1172/JCI10458.
[31] P.-M. Andrault, A.C. Schamberger, T. Chazeirat, D. Sizaret, J. Renault, C.A. Staab-Weijnitz, E. Hennen, A. Petit-Courty, M. Wartenberg, A. Saidi, T. Baranek, S. Guyetant, Y. Courty, O. Eickelberg, G. Lalmanach, F. Lecaille, Cigarette smoke induces overexpression of active human cathepsin S in lungs from current smokers with or without COPD, Am. J. Physiol. Lung Cell Mol. Physiol. (2019). https://doi.org/10.1152/ajplung.00061.2019.
[32] D.F. Doherty, S. Nath, J. Poon, R.F. Foronjy, M. Ohlmeyer, A.J. Dabo, M. Salathe, M. Birrell, M. Belvisi, N. Baumlin, M.D. Kim, S. Weldon, C. Taggart, P. Geraghty, Protein Phosphatase 2A Reduces Cigarette Smoke-induced Cathepsin S and Loss of Lung Function, Am. J. Respir. Crit. Care Med. 200 (2019) 51–62. https://doi.org/10.1164/rccm.201808-1518OC.
[33] T. Zheng, M.J. Kang, K. Crothers, Z. Zhu, W. Liu, C.G. Lee, L.A. Rabach, H.A. Chapman, R.J. Homer, D. Aldous, G.T. De Sanctis, G. Desanctis, S. Underwood, M. Graupe, R.A. Flavell, J.A. Schmidt, J.A. Elias, Role of cathepsin S-dependent epithelial cell apoptosis in IFN-gamma-induced alveolar remodeling and pulmonary emphysema, J. Immunol. 174 (2005) 8106–8115.

[34] M. Kasabova, A. Saidi, C. Naudin, J. Sage, F. Lecaille, G. Lalmanach, Cysteine Cathepsins: Markers and Therapy Targets in Lung Disorders, Clinic. Rev. Bone Miner. Metab. 9 (2011) 148–161. https://doi.org/10.1007/s12018-011-9094-6.
[35] J.J.M. Wiener, S. Sun, R.L. Thurmond, Recent advances in the design of cathepsin S inhibitors, Curr. Top. Med. Chem. 10 (2010) 717–732. https://doi.org/10.2174/156802610791113432.
[36] N.M. Giles, A.B. Watts, G.I. Giles, F.H. Fry, J.A. Littlechild, C. Jacob, Metal and redox modulation of cysteine protein function, Chem. Biol. 10 (2003) 677–693.
[37] G. Roos, J. Messens, Protein sulfenic acid formation: from cellular damage to redox regulation, Free Radic. Biol. Med. 51 (2011) 314–326. https://doi.org/10.1016/j.freeradbiomed.2011.04.031.
[38] V. Gupta, K.S. Carroll, Sulfenic acid chemistry, detection and cellular lifetime, Biochim. Biophys. Acta. 1840 (2014) 847–875. https://doi.org/10.1016/j.bbagen.2013.05.040.
[39] C.L. Hawkins, M.J. Davies, Detection, identification, and quantification of oxidative protein modifications, J. Biol. Chem. 294 (2019) 19683–19708. https://doi.org/10.1074/jbc.REV119.006217.
[40] M.E. McGrath, J.T. Palmer, D. Brömme, J.R. Somoza, Crystal structure of human cathepsin S, Protein Sci. 7 (1998) 1294–1302. https://doi.org/10.1002/pro.5560070604.
[41] J.A. Rullmann, M.N. Bellido, P.T. van Duijnen, The active site of papain. All-atom study of interactions with protein matrix and solvent, J. Mol. Biol. 206 (1989) 101–118.
[42] E. Godat, V. Hervé-Grépinet, F. Veillard, F. Lecaille, M. Belghazi, D. Brömme, G. Lalmanach, Regulation of cathepsin K activity by hydrogen peroxide, Biol. Chem. 389 (2008) 1123–1126. https://doi.org/10.1515/BC.2008.109.
[43] T.D. Lockwood, Cys-His proteases are among the wired proteins of the cell, Arch. Biochem. Biophys. 432 (2004) 12–24. https://doi.org/10.1016/j.abb.2004.09.011.
[44] H.A. Headlam, M. Gracanin, K.J. Rodgers, M.J. Davies, Inhibition of cathepsins and related proteases by amino acid, peptide, and protein hydroperoxides, Free Radic. Biol. Med. 40 (2006) 1539–1548. https://doi.org/10.1016/j.freeradbiomed.2005.12.036.
[45] V. Borutaite, G.C. Brown, Caspases are reversibly inactivated by hydrogen peroxide, FEBS Lett. 500 (2001) 114–118.
[46] J. Sage, F. Mallèvre, F. Barbarin-Costes, S.A. Samsonov, J.-P. Gehrcke, M.T. Pisabarro, E. Perrier, S. Schnebert, A. Roget, T. Livache, C. Nizard, G. Lalmanach, F. Lecaille, Binding of chondroitin 4-sulfate to cathepsin S regulates its enzymatic activity, Biochemistry. 52 (2013) 6487–6498. https://doi.org/10.1021/bi400925g.
[47] G. Kramer, A. Paul, A. Kreusch, S. Schüler, B. Wiederanders, K. Schilling, Optimized folding and activation of recombinant procathepsin L and S produced in Escherichia coli, Protein Expr. Purif. 54 (2007) 147–156. https://doi.org/10.1016/j.pep.2007.02.007.
[48] T. Garenne, A. Saidi, B.F. Gilmore, E. Niemiec, V. Roy, L.A. Agrofoglio, M. Kasabova, F. Lecaille, G. Lalmanach, Active site labeling of cysteine cathepsins by a straightforward diazomethylketone probe derived from the N-terminus of human cystatin C, Biochem. Biophys. Res. Commun. 460 (2015) 250–254. https://doi.org/10.1016/j.bbrc.2015.03.020.
[49] J. Qian, C. Klomsiri, M.W. Wright, S.B. King, A.W. Tsang, L.B. Poole, C.M. Furdui, Simple synthesis of 1,3-cyclopentanedione derived probes for labeling sulfenic acid proteins, Chem. Commun. 47 (2011) 9203–9205. https://doi.org/10.1039/c1cc12127h.
[50] M. Lo Conte, J. Lin, M.A. Wilson, K.S. Carroll, A Chemical Approach for the Detection of Protein Sulfinylation, ACS Chem. Biol. 10 (2015) 1825–1830. https://doi.org/10.1021/acschembio.5b00124.
[51] A.C. Schamberger, N. Mise, J. Jia, E. Genoyer, A.Ö. Yildirim, S. Meiners, O. Eickelberg, Cigarette smoke-induced disruption of bronchial epithelial tight junctions is prevented by transforming growth factor-β, Am. J. Respir. Cell Mol. Biol. 50 (2014) 1040–1052. https://doi.org/10.1165/rcmb.2013-0090OC.
[52] J. Dairou, B. Pluvinage, J. Noiran, E. Petit, J. Vinh, I. Haddad, J. Mary, J.-M. Dupret, F. Rodrigues-Lima, Nitration of a critical tyrosine residue in the allosteric inhibitor site of muscle glycogen phosphorylase impairs its catalytic activity, J. Mol. Biol. 372 (2007) 1009–1021. https://doi.org/10.1016/j.jmb.2007.07.011.

[53] B. Turk, I. Dolenc, V. Turk, J.G. Bieth, Kinetics of the pH-induced inactivation of human cathepsin L, Biochemistry. 32 (1993) 375–380.
[54] D. Brömme, P.R. Bonneau, P. Lachance, A.C. Storer, Engineering the S2 subsite specificity of human cathepsin S to a cathepsin L- and cathepsin B-like specificity, J. Biol. Chem. 269 (1994) 30238–30242.
[55] D.P. Klose, B.A. Wallace, R.W. Janes, 2Struc: the secondary structure server, Bioinformatics. 26 (2010) 2624–2625. https://doi.org/10.1093/bioinformatics/btq480.
[56] R.B. Holt, C.K. McLane, O. Oldenberg, Ultraviolet Absorption Spectrum of Hydrogen Peroxide, J. Chem. Phys. 16 (1948) 225–229. https://doi.org/10.1063/1.1746843.
[57] H. Fischer, J.H. Widdicombe, Mechanisms of acid and base secretion by the airway epithelium, J. Membr. Biol. 211 (2006) 139–150. https://doi.org/10.1007/s00232-006-0861-0.
[58] S.I. Rennard, Cigarette smoke in research, Am. J. Respir. Cell Mol. Biol. 31 (2004) 479–480. https://doi.org/10.1165/rcmb.F284.
[59] Z. Li, W.S. Hou, D. Brömme, Collagenolytic activity of cathepsin K is specifically modulated by cartilage-resident chondroitin sulfates, Biochemistry. 39 (2000) 529–536. https://doi.org/10.1021/bi992251u.
[60] I. Dalle-Donne, D. Giustarini, R. Colombo, R. Rossi, A. Milzani, Protein carbonylation in human diseases, Trends Mol. Med. 9 (2003) 169–176.
[61] J. Dairou, N. Atmane, F. Rodrigues-Lima, J.-M. Dupret, Peroxynitrite irreversibly inactivates the human xenobiotic-metabolizing enzyme arylamine N-acetyltransferase 1 (NAT1) in human breast cancer cells: a cellular and mechanistic study, J. Biol. Chem. 279 (2004) 7708–7714. https://doi.org/10.1074/jbc.M311469200.
[62] A.J. Väänänen, E. Kankuri, P. Rauhala, Nitric oxide-related species-induced protein oxidation: reversible, irreversible, and protective effects on enzyme function of papain, Free Radic. Biol. Med. 38 (2005) 1102–1111. https://doi.org/10.1016/j.freeradbiomed.2005.01.007.
[63] M.D. Percival, M. Ouellet, C. Campagnolo, D. Claveau, C. Li, Inhibition of cathepsin K by nitric oxide donors: evidence for the formation of mixed disulfides and a sulfenic acid, Biochemistry. 38 (1999) 13574–13583.
[64] S. Mohr, B. Zech, E.G. Lapetina, B. Brüne, Inhibition of caspase-3 by S-nitrosation and oxidation caused by nitric oxide, Biochem. Biophys. Res. Commun. 238 (1997) 387–391. https://doi.org/10.1006/bbrc.1997.7304.
[65] M. Josephs, M. Katan, F. Rodrigues-Lima, Irreversible inactivation of magnesium-dependent neutral sphingomyelinase 1 (NSM1) by peroxynitrite, a nitric oxide-derived oxidant, FEBS Lett. 531 (2002) 329–334.
[66] O. Quraishi, A.C. Storer, Identification of internal autoproteolytic cleavage sites within the prosegments of recombinant procathepsin B and procathepsin S. Contribution of a plausible unimolecular autoproteolytic event for the processing of zymogens belonging to the papain family, J. Biol. Chem. 276 (2001) 8118–8124. https://doi.org/10.1074/jbc.M005851200.
[67] J.R. Pungercar, D. Caglic, M. Sajid, M. Dolinar, O. Vasiljeva, U. Pozgan, D. Turk, M. Bogyo, V. Turk, B. Turk, Autocatalytic processing of procathepsin B is triggered by proenzyme activity, FEBS J. 276 (2009) 660–668. https://doi.org/10.1111/j.1742-4658.2008.06815.x.
[68] G. Lalmanach, E. Diot, E. Godat, F. Lecaille, V. Hervé-Grépinet, Cysteine cathepsins and caspases in silicosis, Biol. Chem. 387 (2006) 863–870. https://doi.org/10.1515/BC.2006.109.

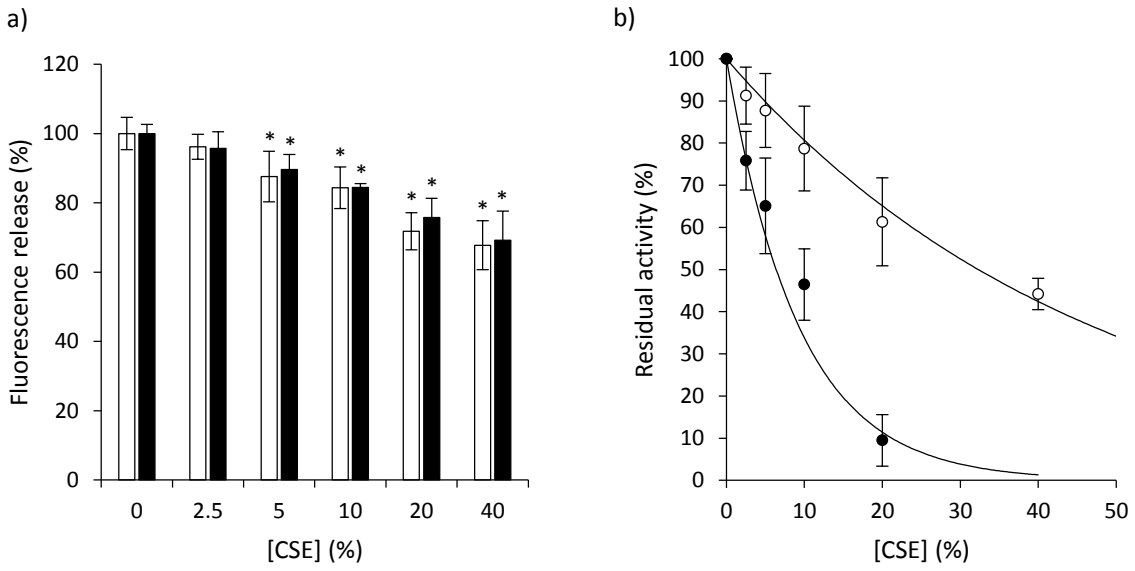
a)
Fluorescence release (%)
120
100
80
60
40
20
0
0
2.5
5
10
20
40
[CSE] (%)
*
b)
Residual activity (%)
100
90
80
70
60
50
40
30
20
10
0
0
10
20
30
40
50
[CSE] (%)

a)

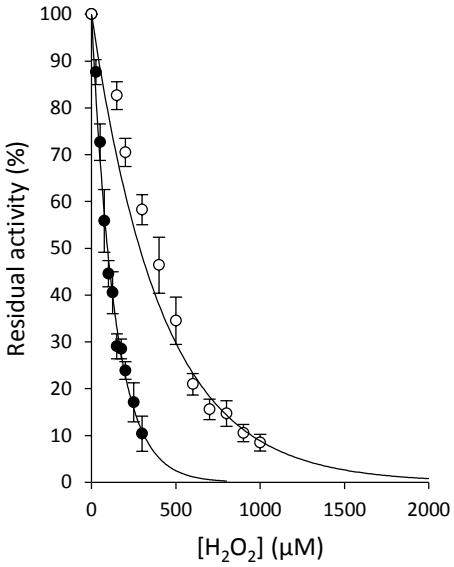
Residual activity (%)
100
90
80
70
60
50
40
30
20
10
0
0
500
1000
1500
2000
[H2O2] (µM)

b)

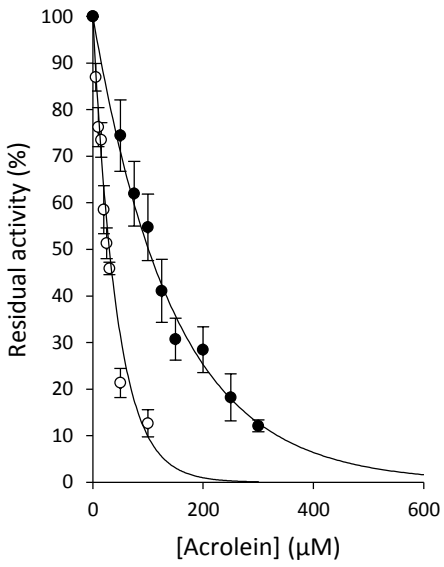
Residual activity (%)
100
90
80
70
60
50
40
30
20
10
0
0
200
400
600
[Acrolein] (µM)

c)

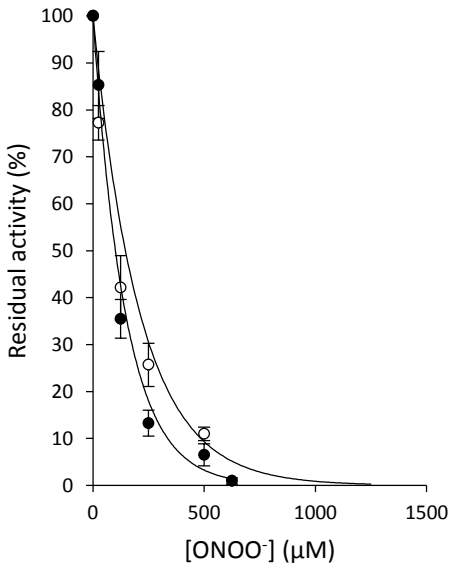
Residual activity (%)
100
90
80
70
60
50
40
30
20
10
0
0
500
1000
1500
[ONOO-] (µM)

d)

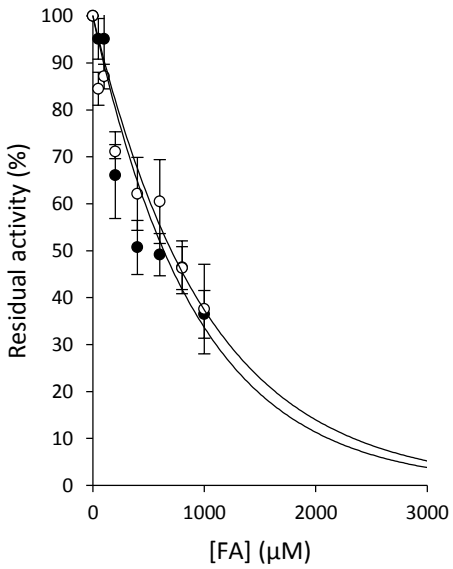
Residual activity (%)
100
90
80
70
60
50
40
30
20
10
0
0
1000
2000
3000
[FA] (µM)

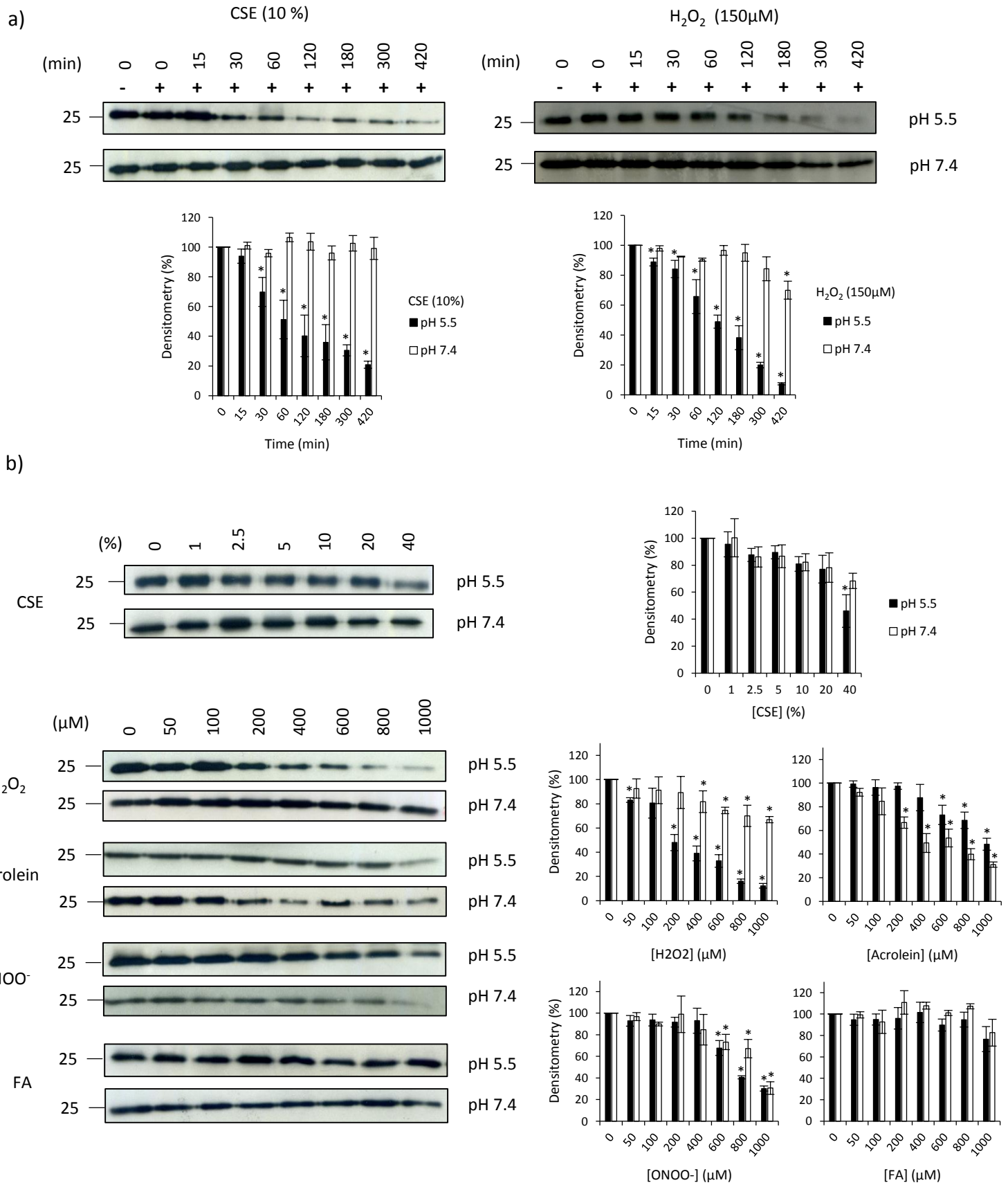
a)
CSE (10 %)
$H_2O_2$ (150µM)
(min)
0 0 15 30 60 120 180 300 420
- + + + + + + + +
25
pH 5.5
pH 7.4
Densitometry (%)
Time (min)
CSE (10%)
$H_2O_2$ (150µM)
b)
(%)
0 1 2.5 5 10 20 40
CSE
[CSE] (%)
(µM)
0 50 100 200 400 600 800 1000
$H_2O_2$
Acrolein
$ONOO^-$
FA
[H2O2] (µM)
[Acrolein] (µM)
[ONOO-] (µM)
[FA] (µM)

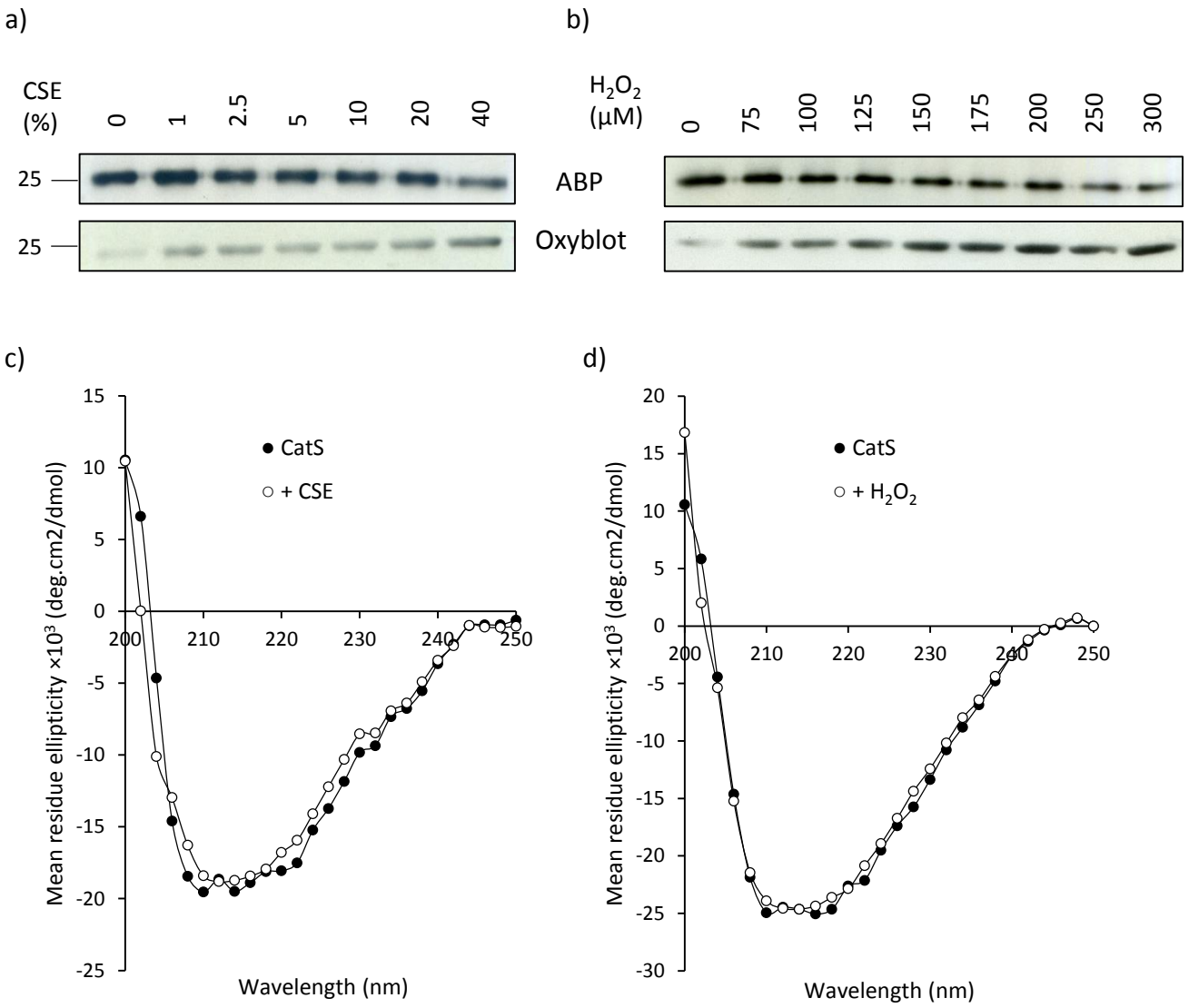
a)
CSE (%)
0
1
2.5
5
10
20
40
25
25
b)
$H_2O_2$ (µM)
0
75
100
125
150
175
200
250
300
ABP
Oxyblot
c)
CatS
+ CSE
Mean residue ellipticity ×10³ (deg.cm2/dmol)
Wavelength (nm)
d)
CatS
+ $H_2O_2$
Mean residue ellipticity ×10³ (deg.cm2/dmol)
Wavelength (nm)

a)

| | Reversibility (%) | | | |
|---|---|---|---|---|
| | pH 5.5 | | pH 7.4 | |
| $H_2O_2$ | (25 - 200 µM) | 24 ± 2 | (200 - 500 µM) | 20 ± 3 |
| Acrolein | (100 - 300 µM) | 2 ± 2 | (10 - 30 µM) | 4 ± 3 |
| $ONOO^-$ | 1250 µM | 10 ± 2 | 1250 µM | 8 ± 1 |
| | 125 µM | 36 ± 5 | 125 µM | 42 ± 3 |

N. I. : No inactivation

b)

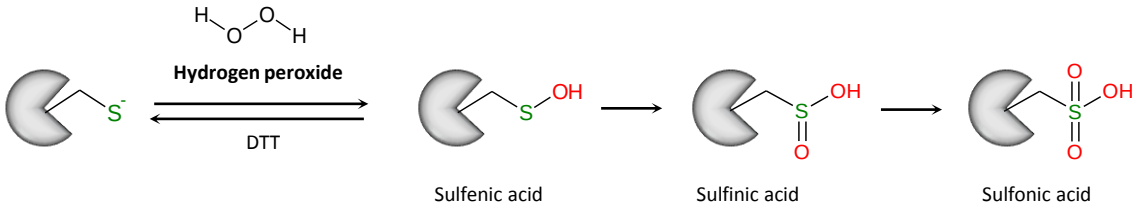


c)

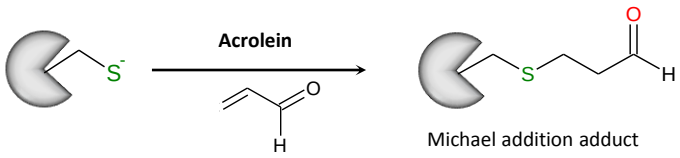


d)

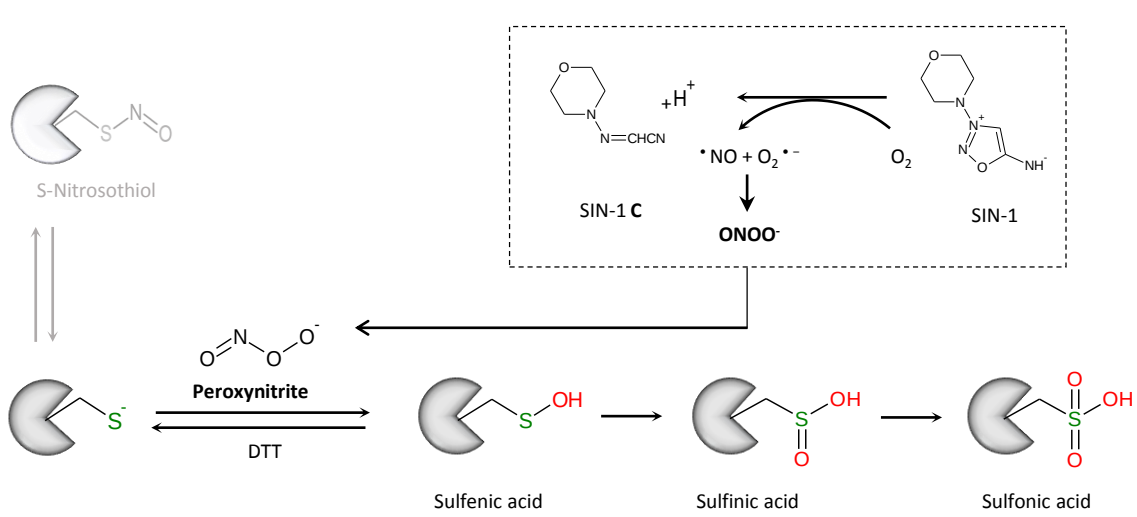

a)

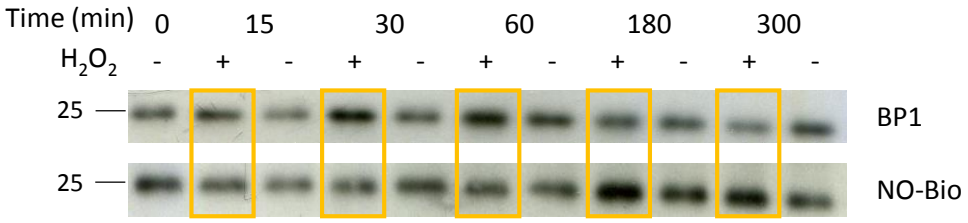


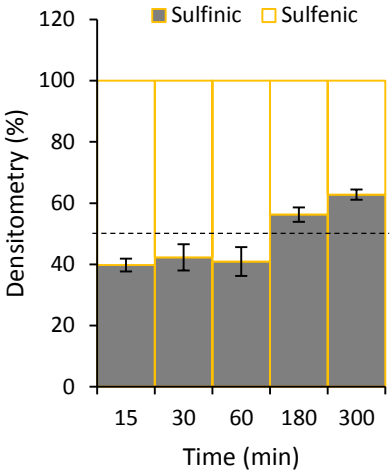


b)

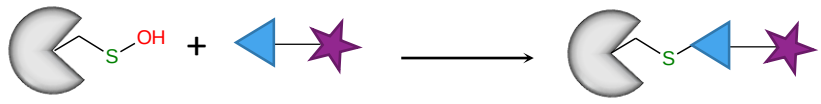


Sulfenic acid

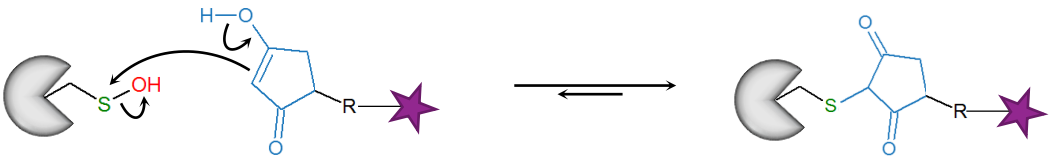


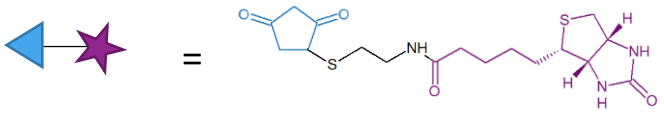


**Sulfenic acid trap** **Biotin**

c)

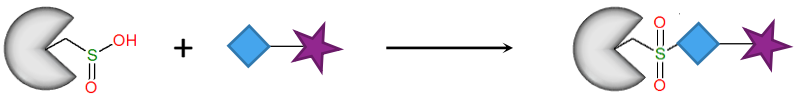


Sulfinic acid

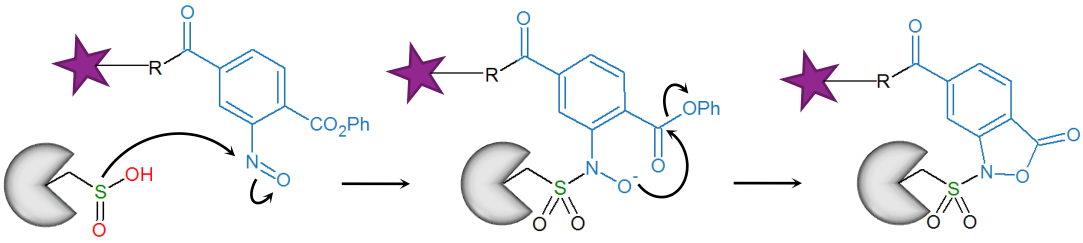


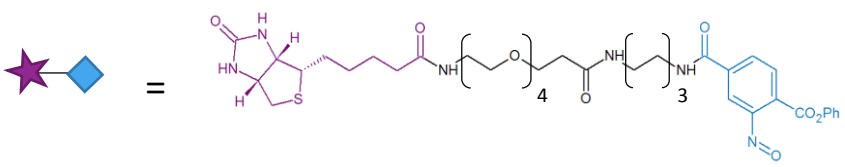


**Biotin** **Sulfinic acid trap**

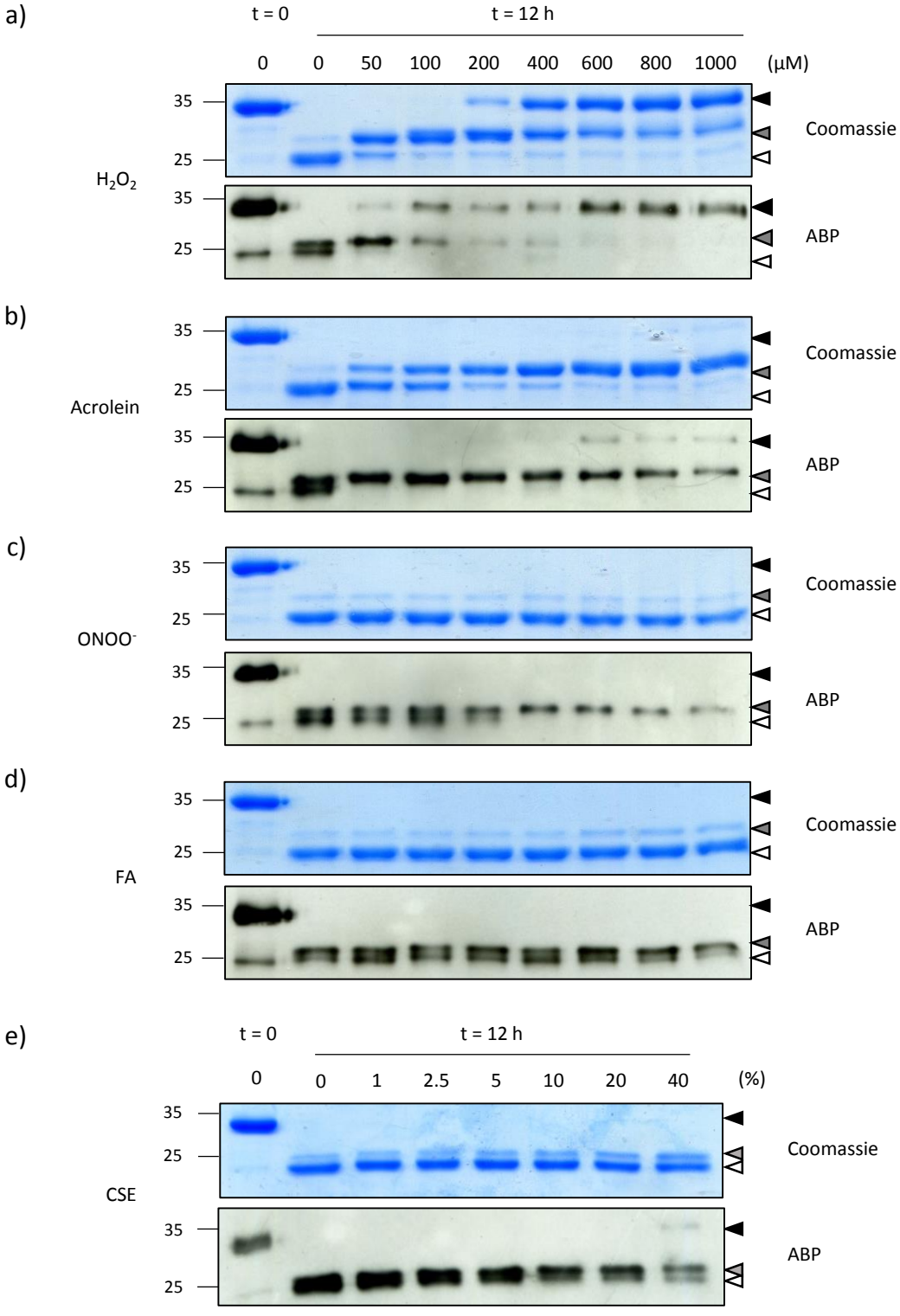
a)
t = 0
t = 12 h
0
0
50
100
200
400
600
800
1000
(µM)
35
25
H2O2
Coomassie
ABP
b)
Acrolein
c)
ONOO-
d)
FA
e)
0
1
2.5
5
10
20
40
(%)
CSE

**Table I**

*Determinations of second-order rate constants*

| | $k_{inact}/[I]$ ($M^{-1}.s^{-1}$) | |
|---|---|---|
| | pH 5.5 | pH 7.4 |
| FA | 0.6 ± 0.2 | 0.5 ± 0.1 |
| $ONOO^-$ | 4.0 ± 1.6 | 4.9 ± 0.8 |
| Acrolein | 4.4 ± 0.4 | 39.7 ± 10.5 |
| $H_2O_2$ | 33.0 ± 2.0 | 4.4 ± 2.2 |

Determinations of second-order rate constants for inactivation of CatS were described in the Materials and Methods section. All kinetic measurements were performed in triplicate and were representative of three independent experiments. Data were represented as the mean ± SEM (n=3).


Cat S